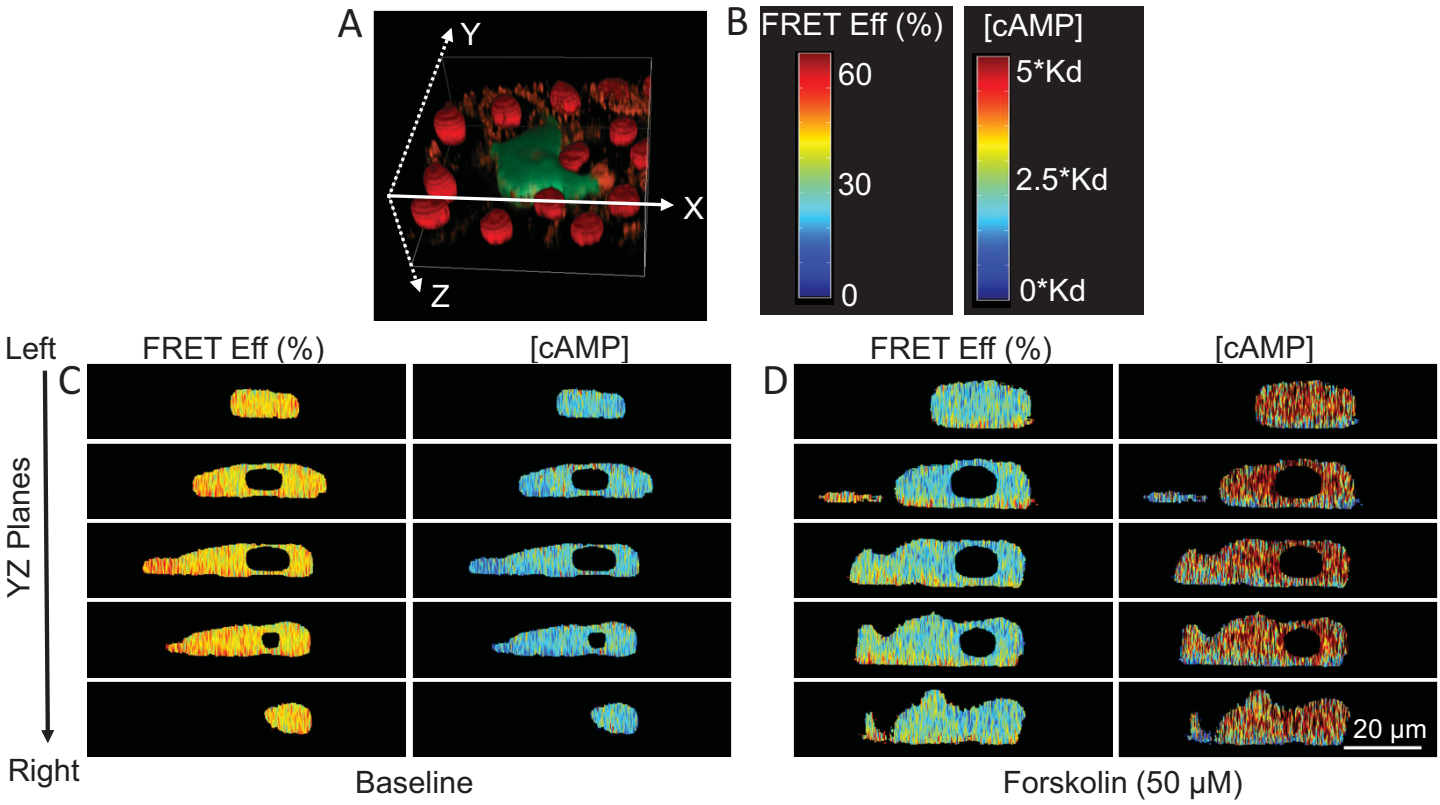
A
Y
X
Z
B
FRET Eff (%)
60
30
0
[cAMP]
5*Kd
2.5*Kd
0*Kd
Left
C
FRET Eff (%)
[cAMP]
YZ Planes
Right
Baseline
D
FRET Eff (%)
[cAMP]
20 µm
Forskolin (50 µM)

Figure S1: FRET efficiencies and [cAMP] from 5 slices in the YZ plane through a single pulmonary microvascular endothelial cell (PMVEC). (A) 3D depiction of a cell expressing the H188 cAMP probe. (B) The color bars depicting the FRET efficiency and [cAMP] color scales for resliced images. (C) YZ slices are displayed from top-to-bottom corresponding as left -to- right in the cell. As in Figure 9, minimal FRET and [cAMP] spatial gradients were observed at baseline conditions. (D) Treatment with 50 µM forskolin for 10 minutes triggered pronounced spatial gradients in FRET efficiency and [cAMP] from the apical to basolateral face of the cell. These data demonstrate the potential for 4D spectral approaches to measure the intracellular distribution of second messenger signals. The scale bar (lower right panel) indicates 20 µm.

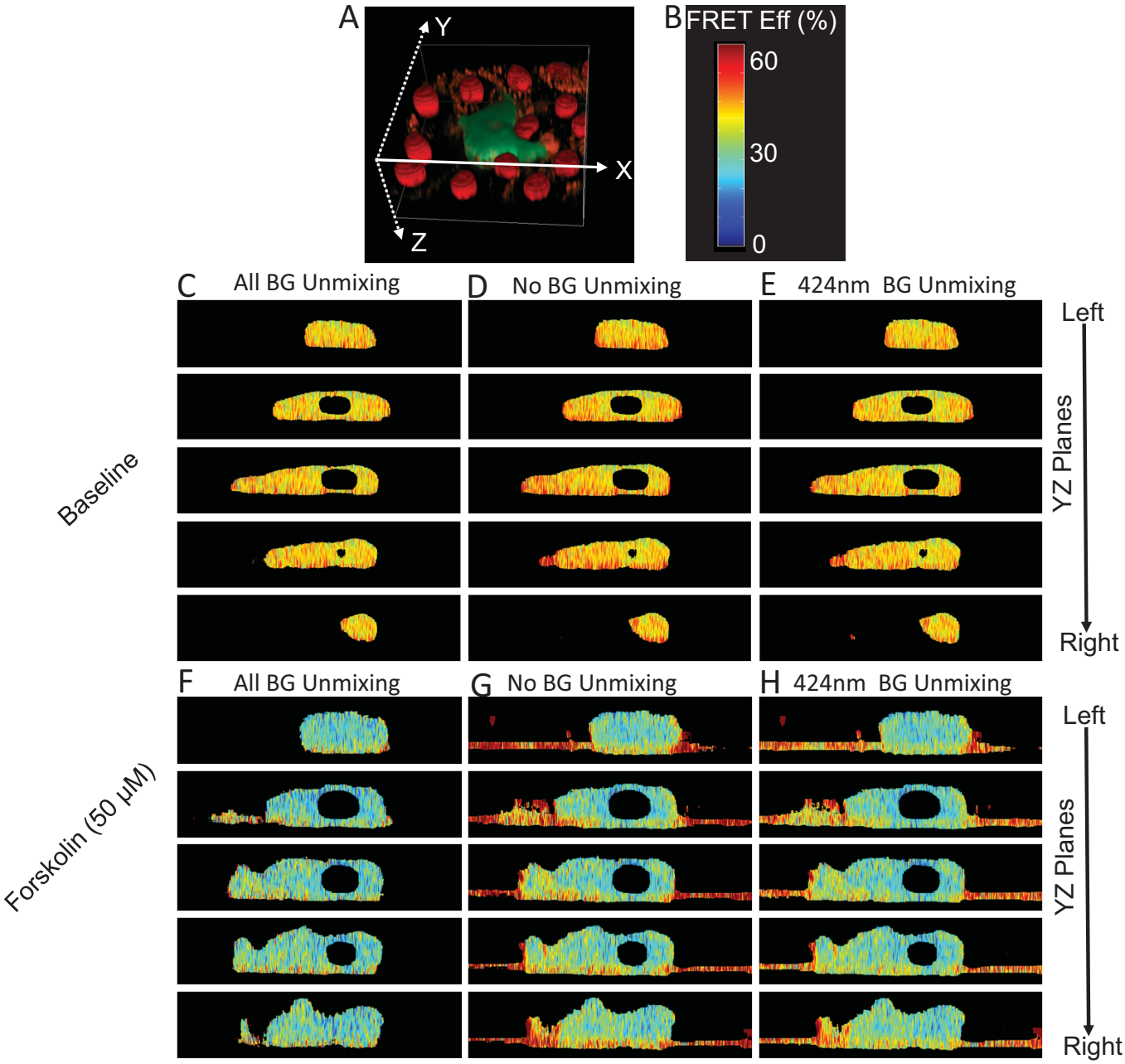
A
Y
X
Z
B
FRET Eff (%)
60
30
0
C All BG Unmixing
D No BG Unmixing
E 424nm BG Unmixing
Baseline
Left
YZ Planes
Right
F All BG Unmixing
G No BG Unmixing
H 424nm BG Unmixing
Forskolin (50 μM)
Left
YZ Planes
Right

Figure S2: Comparison of FRET maps obtained using libraries with all background components (panels C and F), no background components (D and G), and only the 424 nm BG component (E and F). Panels C, D, E represent the FRET maps at baseline and panels F, G, H represent the FRET maps at 10 minutes after forskolin treatment. Notice that the results from unmixing with no background components or only 1 background component indicate an inability to separate basolateral autofluorescence from the cell, likely associated with ECM, from the cell (panels G and H), whereas the results from unmixing with all background components show a clean separation between the cell and underlying autofluorescence (panel F).

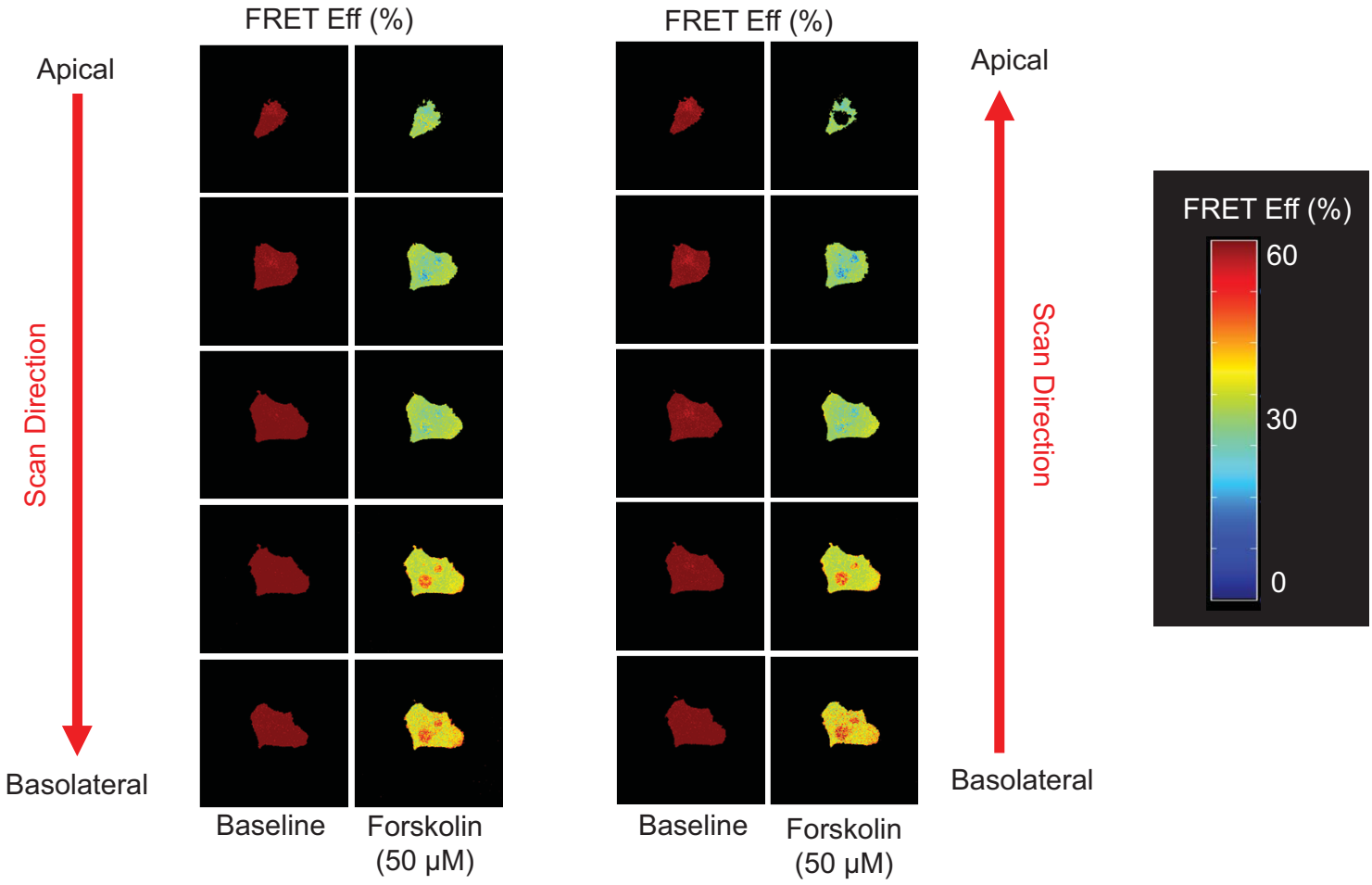
FRET Eff (%)
Apical
Scan Direction
Basolateral
Baseline
Forskolin
(50 μM)
FRET Eff (%)
Apical
Scan Direction
Basolateral
Baseline
Forskolin
(50 μM)
FRET Eff (%)
60
30
0

Figure S3: FRET efficiencies at baseline and after 50 µM forskolin treatment of a PMVEC visualized in five XY planes. In this experiment, imaging of the Z stack was initiated in two directions: (i) at the top of the cell with subsequent scans of lower slices (toward the bottom of the cell) - first and second columns;(ii) atbottom of the cell and with subsequent scans of higher slices (towards the top of the cell) - third and fourth columns. Color bars indicate the magnitude of FRET efficiency. Data were resliced in the XY plane. FRET distributions are shown for five slices. FRET efficiency under baseline and forskolin treatment conditions are indicated in the adjacent panels. The baseline FRET efficiency is high, indicating little or no FRET/cAMP gradient. Following 10 minute treatment with 50 µM forskolin, the FRET efficiency was reduced. Small spatial gradients in FRET and [cAMP] were observed from the apical to basolateral face of the cell. The development of gradients is same in either of the scan directions and does not depend on whether the scan was initiated at the top of the cell or the bottom of the cell. This demonstrated that gradients were not artifacts induced by the order in which Z-slices were acquired.

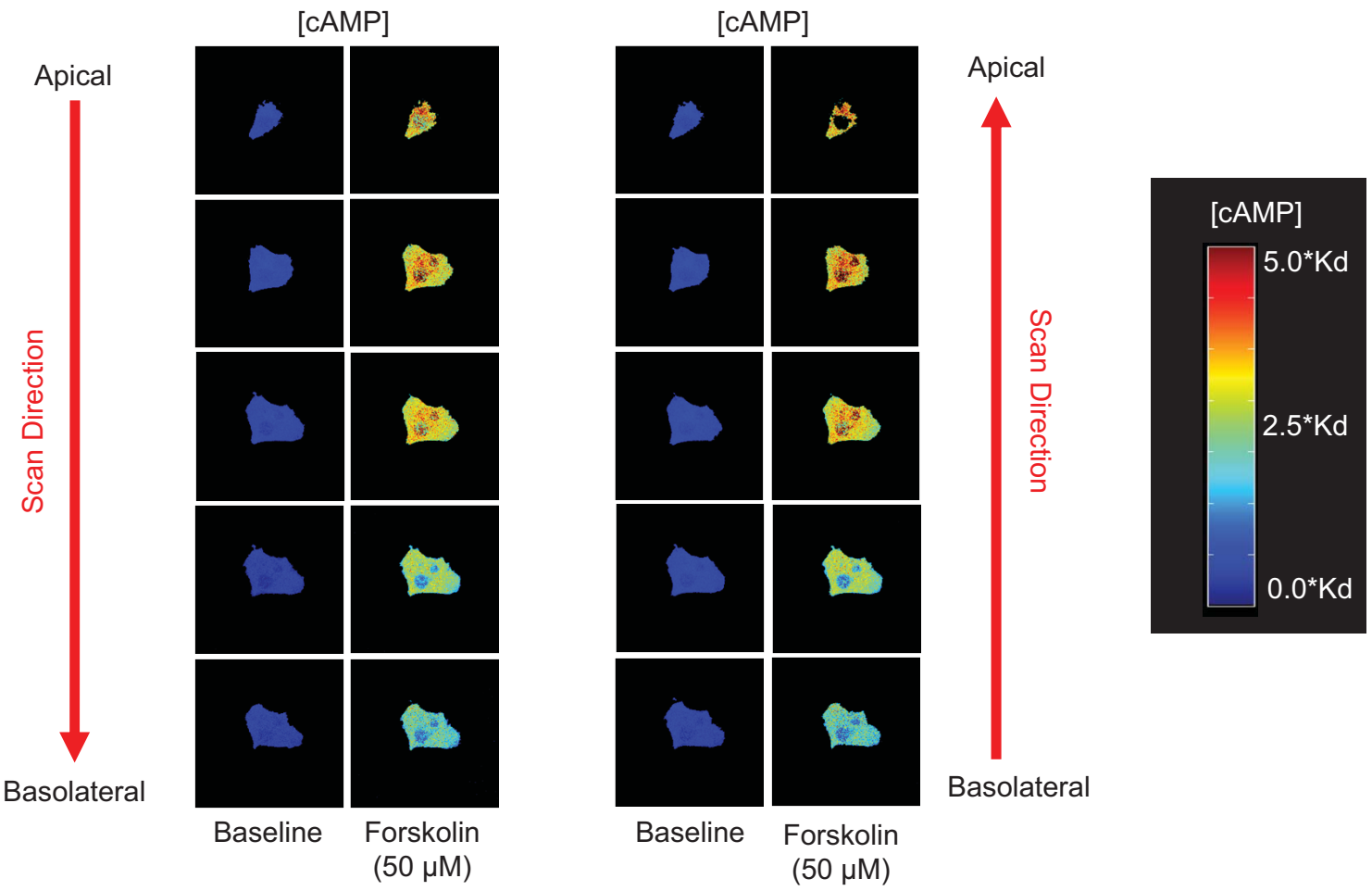
[cAMP]
Apical
Scan Direction
Basolateral
Baseline
Forskolin
(50 μM)
[cAMP]
Apical
Scan Direction
Basolateral
Baseline
Forskolin
(50 μM)
[cAMP]
5.0*Kd
2.5*Kd
0.0*Kd

Figure S4: [cAMP] at baseline and after 50 µM forskolin treatment of a PMVEC visualized in five XY planes. FRET efficiencies in Figure S1were mapped to [cAMP] as described in the Material and Methods. Consistent with changes in FRET efficiencies shown in Figure S1, [cAMP] changed upon treatment with forskolin. First and second columnsshow [cAMP] at baseline and after forskloin treatment in which the image scan was initiated at top of the cell. Third and fourth columns represent changes in [cAMP] at baseline and after treatment in which the image scans were initiated at bottom of the cell. The development of cAMP gradients weresimilar in either of the scan direction and did not depend on where scans were initiated. This demonstrated that the gradients were not artifacts induced by the order in which Z-slices were acquired. Color bars indicate the [cAMP].

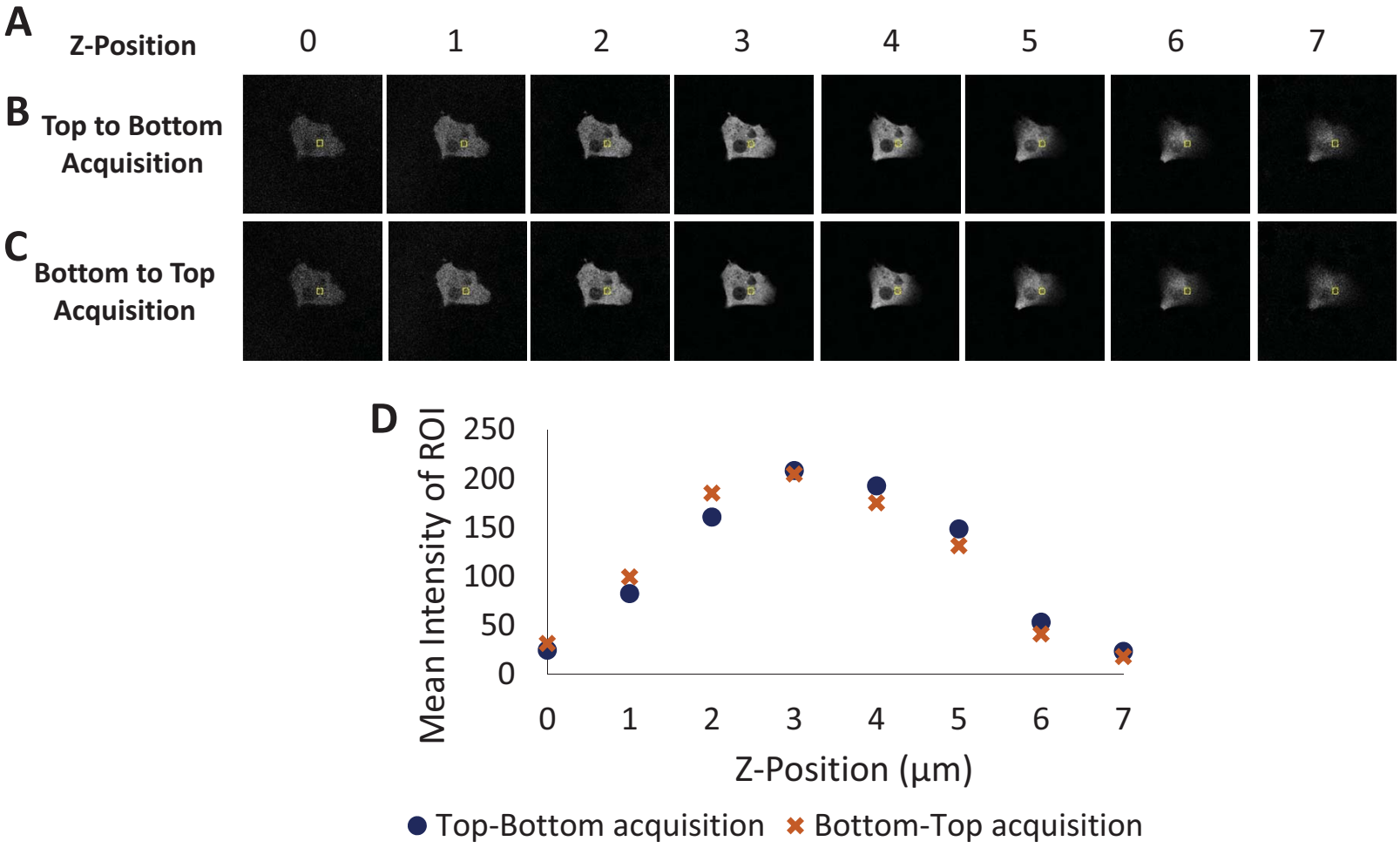
A
Z-Position
0
1
2
3
4
5
6
7
B
Top to Bottom Acquisition
C
Bottom to Top Acquisition
D
Mean Intensity of ROI
250
200
150
100
50
0
0
1
2
3
4
5
6
7
Z-Position (µm)
Top-Bottom acquisition
Bottom-Top acquisition

Figure S5: To account for photobleaching, the unmixed donor images from basolateral face to the apical face (represented as 0 to 7 in panel A) obtained from top-bottom z-stack scan (panel B) and bottom-top z-stack scan (pane C). A region of interest, shown as a yellow square is considered and mean intensity in the region is measured. The mean intensity is plotted against the Z-position (from bottom to top) (D). As observed in the plot, negligible or minimal photobleaching is observed.

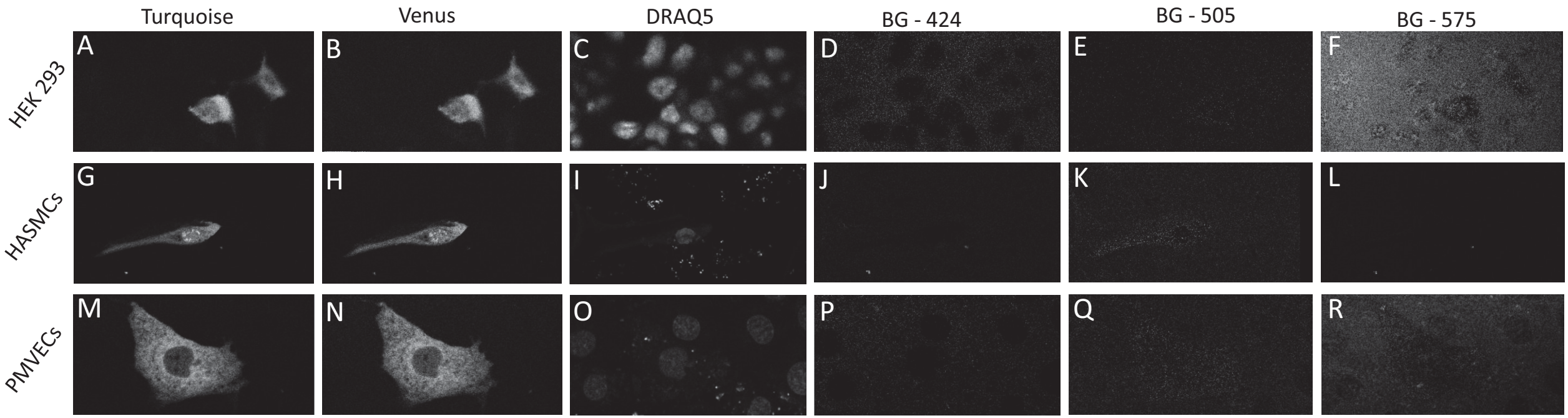
Turquoise
Venus
DRAQ5
BG - 424
BG - 505
BG - 575
HEK 293
HASMCs
PMVECs
A
B
C
D
E
F
G
H
I
J
K
L
M
N
O
P
Q
R

Figure S6: Spectral FRET analysis using common background signatures in three different cell types - Human embryonic kidney cells (HEK 293), human airway smooth muscle cells (HASMCs), and rat pulmonary microvascular endothelial cells (PMVECs). For all cell lines, cells were transfected with the H188 FRET reporter and imaged under similar settings. (A-F) Unmixed images of Turquoise, Venus, DRAQ5, and 3 background signatures with characteristic peaks at 424, 505, and 575 nm, labeled in HEK 293 cells. (J-L) Unmixed images of the same components labeled in HASMCs. (P-Q) Unmixed images of the same components labeled in PMVECs. As can be seen in all 3 cell lines, at least one of the background components is present at non-negligible levels, especially considering the sensitivity of FRET efficiency calculations to background or noise components.

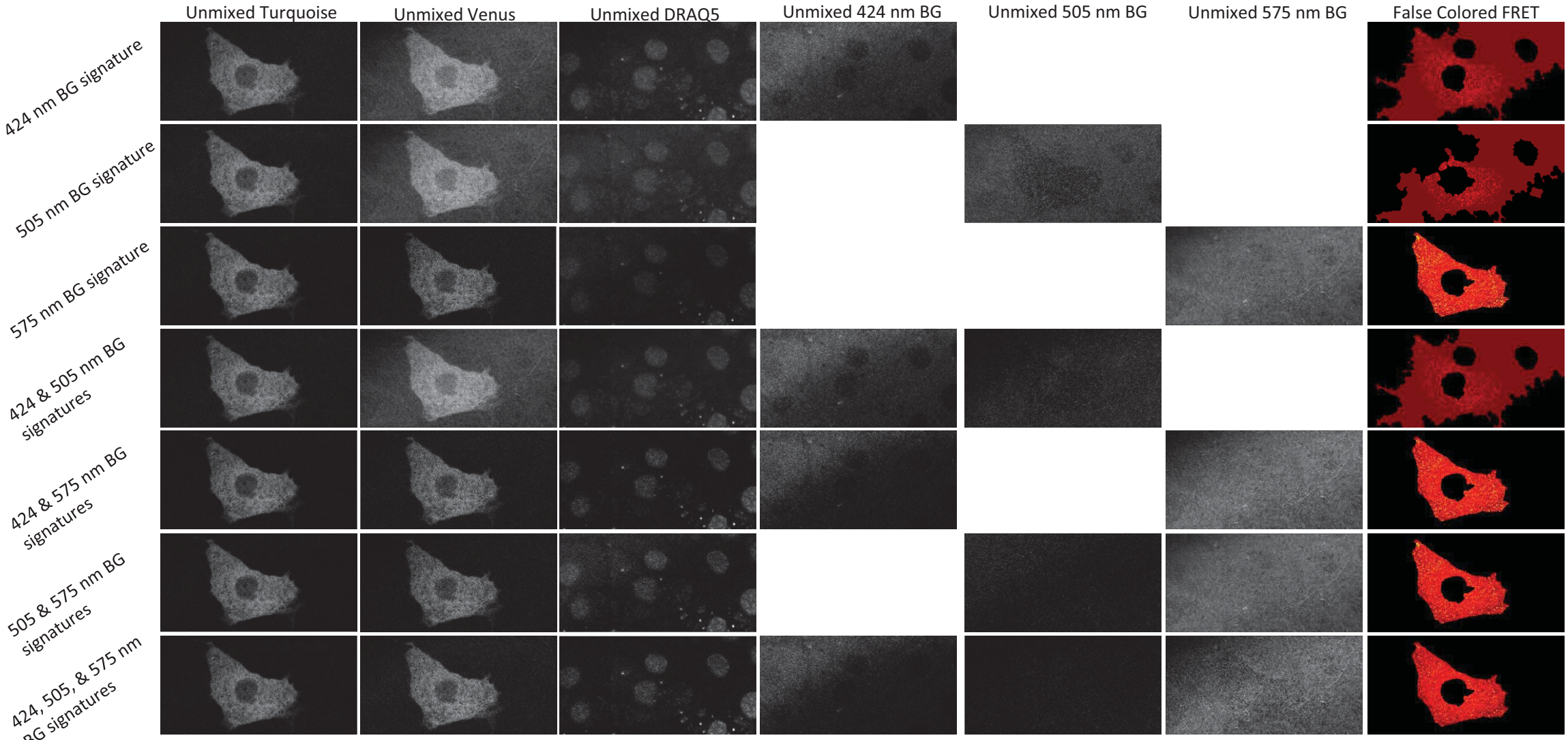
Unmixed Turquoise
Unmixed Venus
Unmixed DRAQ5
Unmixed 424 nm BG
Unmixed 505 nm BG
Unmixed 575 nm BG
False Colored FRET
424 nm BG signature
505 nm BG signature
575 nm BG signature
424 & 505 nm BG signatures
424 & 575 nm BG signatures
505 & 575 nm BG signatures
424, 505, & 575 nm BG signatures

Figure S7: Effects of including different combinations of background signatures on spectral FRET analysis. Row headers indicate which of 3 background signatures were included in the spectral library. Column headers indicate the unmixed endmember image or the calculated and false-colored FRET efficiency image. FRET efficiency colors were selected using the look up table shown in Figure 7.

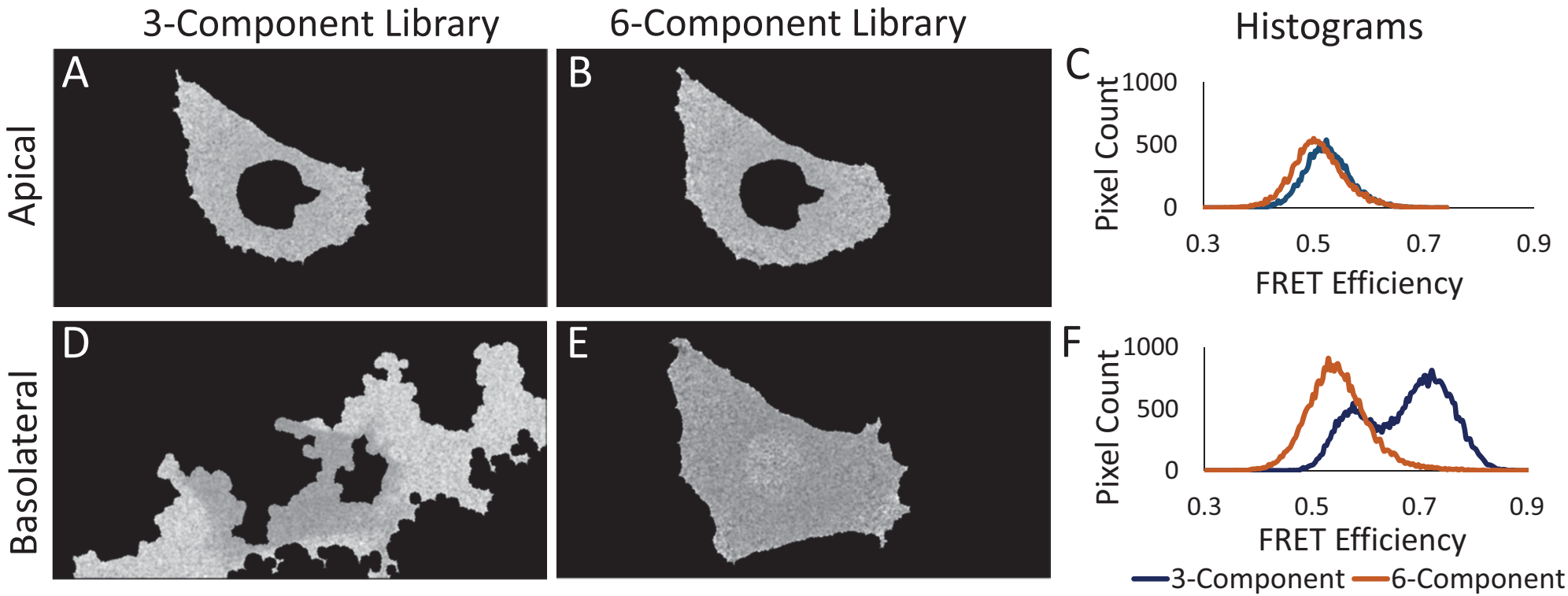
3-Component Library
6-Component Library
Histograms
Apical
Basolateral
A
B
C
D
E
F
Pixel Count
1000
500
0
0.3
0.5
0.7
0.9
FRET Efficiency
3-Component
6-Component

Figure S8: Comparison of histograms (C and F) to show the spread of FRET efficiencies obtained using 3-component (A and D) and 6-component library (B and E). The distribution of FRET efficiency is similar for both 3- and 6- component libraries for the z-slices selected at the apical face of a cell (A, B, and C). However, in contrast, the FRET efficiency is widely distributed in the basolateral slice obtained from 3-component unmixing compared to that of 6-component unmixing (D, E, and F). These suggest the noise is unevenly distributed in axial direction and correction for background is important for the improved FRET analysis.